CHAPTER 1

INTRODUCTION

1.1 BACKGROUND OF STUDY

As the majority of people spend most of their time indoors and often share the same space, knowledge and prediction of the indoor climate conditions is important to optimize the indoor climate for the occupants at the design phase. A gamut of parameters determines the indoor climate and is important for the well-being of the occupant of a room in terms of thermal comfort and (perceived) indoor air quality. This research has focused on two parameters, namely velocity and temperature.

In recent years in literature an overall consensus is found on the fact that thermal comfort is above all a personal experience. This point of departure differs from the established professional attitude to design a uniform climate for a building instead of creating comfort for people. It has lead to a renewed interest for personal control within a building and especially for task conditioning systems. Such systems intend to condition a small space around the occupant, controlled by the occupant.

For the determination and prediction of the indoor air flow pattern two important tools are available: *measurement* and *simulation* (Computational Fluid Dynamics - CFD). Both tools currently however have limitations in accuracy and reliability with which the flow pattern can be determined. In this thesis the best measurement assumption are chose and simulation tool are investigated extensively in order to give a contribution to the reliability with which the indoor climate can be predicted and optimized.

With regard to *simulation*; Prediction of the indoor air flow using the CFD tool is very attractive given the restrictions and effort to measure the flow. Experimental validation of a CFD-model is necessary for a quantitative credibility of the results. The number of accurately described full-scale three dimensional validation studies for indoor air flow however is very limited.

Temperature and velocity measurement data have been obtained for a configuration in which the supply flow rate and the diffuser position were varied. The obtained measurement results have been discussed in relation to results described in literature and were found to be realistic and suitable for comparison with similar numerical simulations.

1.2 PROBLEM STATEMENT

1.2.1 Problem Identification

The main objective of buildings has always been to provide shelter for sun, wind, cold and rain. In the past designs were relatively simple and took into consideration the local environmental conditions. With respect to the indoor climate, passive cooling was provided through natural ventilation and/or thermal mass and additional heating was possible. Often “builder” and “occupant” were one and the same. This meant that issues such as personal comfort were given a high priority.

At the end of the 19^{th} century new building construction technology was introduced. This new technology and materials such as steel made it possible to design higher and deeper buildings. Artificial lighting and ventilation created an indoor climate largely independent of outdoor climate conditions. The increased technological complexity and size of modern buildings lead to specialization in the building industry. As a result buildings very often are not being built around the needs of individual occupants, but for broader functions.

Importance of indoor air flow - To date, most people spend the majority of their time indoors, often in shared spaces. With the introduction of mechanical environmental control systems, and the resulting increased control of the indoor climate, the expectations of the occupant for a thermally comfortable indoor climate have risen.

1.2.2 Significance of the Study

This study is important to find the optimum ventilation system (diffuser position & airflow variation) due to rise of the expectations of the occupant for a thermally comfortable indoor climate.

1.3 OBJECTIVE

In general, the main aim of this research is to show the influence of diffuser position and air flow variation to the room temperature distribution. If the temperature distribution in a room can be improved by finding the right position of diffuser and also air flow variation, then it will be possible to optimize indoor air quality, thermal comfort and energy use during the design phase. The specific objectives of the study are therefore as follows:

- Create a 3-dimensional computational grid with a mesh to predict air flow
- Simulate the air flow using CFD under various condition – different diffuser angle and air velocity
- Investigate the flow and temperature distribution

1.4 SCOPE OF STUDY

This study should therefore consider the three most important methodologies to acquire data that are applied in indoor climate research:

1. Modeling
2. Simulation using CFD
3. Analysis for the simulation result

1.5 RELEVANCY OF THE STUDY

Given the status of indoor climate research described above and the obvious importance of good indoor environmental conditions, this research is needed to bring the room temperature distribution to the fore.

CHAPTER 2

LITERATURE REVIEW

This section provides a further elaboration of the subjects to be investigated in this study. This includes a discussion of the status of indoor environmental research and ventilation strategies.

2.1 VENTILATION TECHNIQUES

The number of indoor air flow configurations is very large. Selecting the right strategy to ventilate a room is dependent on many factors including the function of the building. This work focuses on mechanical ventilation in office buildings.

Two main principles are available for mechanical ventilation of an office room: (1) mixing ventilation and (2) displacement ventilation. Mixing ventilation means that the air is supplied to the room at relatively high velocity. The entrainment of room air in the supply jet causes a high degree of mixing to take place. As a result the temperature and contaminant concentration tends to remain uniform. Mixing ventilation has been the most important ventilation principle since the introduction of mechanical ventilation (Carrier 1965) [1].

With displacement ventilation relatively cool and clean air is supplied at floor level at a low velocity. Air from the lower part of the room is induced upward by rising convection flows from heat sources in the room and then is removed at ceiling level. The air velocities in the room are very low. A distinct characteristic of displacement ventilation is the vertical temperature and contaminant concentration gradient, with a sharp horizontal interface between the lower relatively clean and fresh air layer and the upper air layer which is relatively warm and contaminated. Displacement

ventilation is only applicable in cooling situations. It was introduced for office environments in the early 80's (Mundt 1996) [2].

Figure 1.1 describes the characteristic differences between the two ventilation principles. The left part of the figure shows the flow pattern and to the right is the averaged velocity magnitude, temperature and contaminant concentration as function of the height.

Although the vertical temperature gradient may negatively impact on the thermal comfort requirements, displacement ventilation increases the ventilation effectiveness due to the contaminant concentration gradient. The ventilation effectiveness gives an indication on the effectiveness with which fresh air is supplied to the inhabited zone. Given the improved ventilation effectiveness and the better air quality levels that can be obtained near the occupant in comparison to mixing ventilation at the same amount of supplied air (Brohus 1997), displacement ventilation is increasingly being applied [3].

It is also possible to ventilate a room naturally. This is achieved by refreshing indoor air with outside air through openings in the façade. For office rooms, natural ventilation alone is, also in a moderate climate as in the Netherlands, unable to maintain the high level of indoor air quality required throughout the year. Therefore, especially for larger office buildings, mostly (central) mechanical ventilation is used.

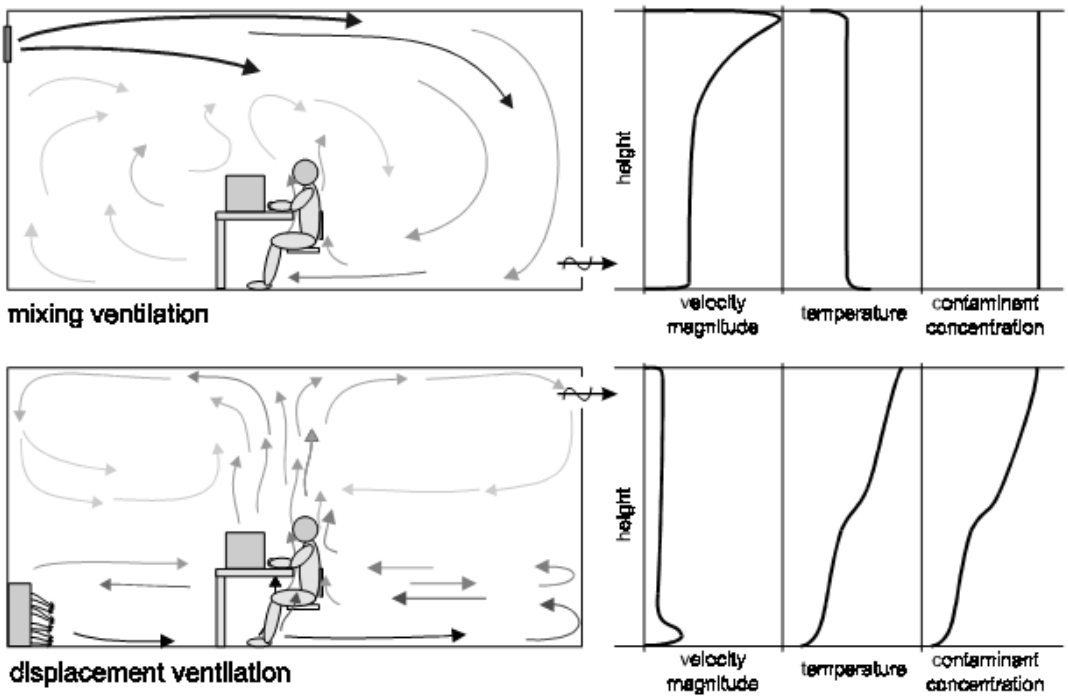

Figure 1.1: Schematized representation of the mixing and displacement ventilation

Centrally controlled air conditioning systems ignore the apparent differences in thermal comfort requirements between persons (Benzinger 1979) [4]. The lack of occupant influence on indoor thermal conditions has increased building related complaints (WHO 1983). These complaints, along with an increasing environmental awareness, has lead to a search for alternatives that allow a more natural way of acclimatizing the indoor environment that also provide more individual control (Hawkes 1996) [5]. This is known as 'bioclimatic design'. In these designs the outdoor climate supports the indoor climate and individual control becomes possible through control of well-thought out façade openings.

Despite this trend to use more natural ventilation, mechanical air conditioning may still be necessary under extreme outdoor climate conditions. In order to achieve thermal comfort, air quality and low energy use, increasing attention is being given to systems which intend to influence only the immediate surroundings of the person operating the system: task conditioning systems (Bauman et al. 1994) [6]. These systems create a micro-climate within a macro-climate (see Figure 1.2). As a result of having local zones, strict comfort-related requirements for the air conditioning of the macro-climate may be mitigated, thereby improving for example, energy efficiency (Bauman and Arens 1996) [7]. Providing individual control of thermal conditions within the micro-zone is seen as the major factor in improving user satisfaction. Therefore, task conditioning systems are considered to be an integral part of the new so-called 'high tech buildings'.

In contrast to mixing and displacement ventilation, the effectiveness of natural ventilation and task conditioning systems is extremely difficult to predict; particularly with today's tools. As a result very little is currently known about the performance of these new innovative systems. Given the strict requirements put in standards (ASHRAE 1992) and the potentially high life cycle costs involved in acclimatizing a building, a reliable prediction of indoor air conditions nevertheless is needed.

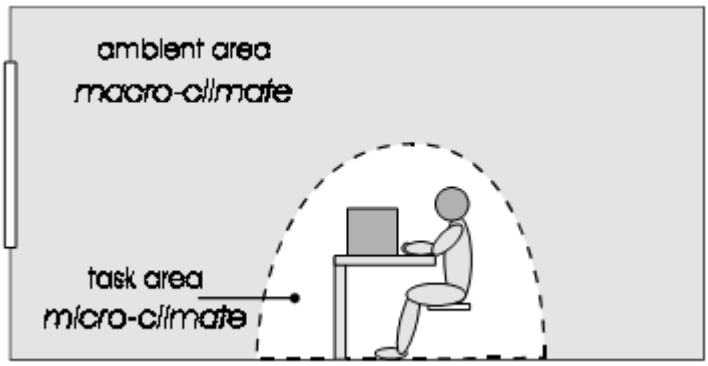

Figure 1.2: Task conditioning principle: micro- versus macro-climate.

2.2 MEASUREMENTS

Data - Data on air velocity and temperature describe the flow field characteristics and are required for numerical validation purposes. Some experimental benchmark studies are available. For example: a two-dimensional isothermal ceiling jet in an enclosure (Nielsen 1974) and a differentially heated cavity with a hot and a cold wall (Cheesewright et al. 1986) [8] [9]. These studies have been used extensively to validate CFD-programs and simulations, but the configurations generally differ from practical indoor air flow problems. Therefore, the measurement of a realistic indoor air flow pattern is necessary to judge the validity of a corresponding CFD-simulation. In order to make a comparison, the data, obtained by measurement or simulation, should be accompanied by the prevailing boundary conditions.

Extensive in-situ measurement series by Thorsauge (1982), Hanzawa et al. (1987) and Melikov et al. (1988 and 1990) provided a better understanding of the actual indoor air flow characteristics [10] [11] [12] [13]. These results however are not suitable for validation purposes as boundary conditions are not known and there are not enough measurements for a single flow pattern.

Other than the Annex 20 ‘Air flow patterns within buildings’ by the International Energy Agency [IEA] (Lemaire 1992) there are very few sources of well documented full-scale indoor air flow measurement results [14]. Given the additional consideration for variation in indoor air flow patterns, the number of full-scale indoor air flow measurements for comparison with, and validation of CFD-simulations is very limited.

Technique - Nearly all of the studies to date applied a hot sphere anemometer to measure the air velocity (Dantec 1985, Crommelin and Dubbeld 1976) [15] [16]. Although this type of anemometer has been especially developed for indoor air flow registration, the signal tends to drift over time and its accuracy depends highly on the application conditions and on regular calibration. In addition, the sensitivity to the calibration conditions and the dynamic characteristics of the sensor are not well-known.

Given the shortcomings of the hot sphere anemometer, there is a great interest to use new measurement techniques. However, the indoor flow characteristics restrict the number of applicable techniques considerably. In order to select the right technique to use, a good overview of the available measurement principles is necessary. However, such an overview does not yet exist.

2.3 SIMULATIONS

Calculating the flow field is attractive in terms of time and costs given the difficulty to determine the flow field experimentally. Numerical models have been developed to allow the study of the stationary and transient characteristics of an air flow pattern with regard to energy use, indoor air quality and thermal comfort. In this introduction a short summary of model concepts is given.

Over the last years CFD has taken a prominent position for simulation of indoor air flow problems. One of its main advantages over other tools is its ability to simulate a wide range of configurations. The development of commercial versions of the CFD-program with extensive data handling possibilities, combined with the rapid increase in computer power, over recent years have further enhanced its practical application. Since its introduction CFD has been applied for a wide range of indoor air flow problems.

A wide range of models is available. Semi-empirical models for the (non-) isothermal jet allows the calculation of a jet extending into a room. These models are based on the boundary layer and turbulence hypotheses. Mass, momentum and energy conservation also forms the basis for semi-empirical models that have been derived to calculate the characteristics of a displacement ventilation flow pattern, especially the convection flow from heat sources and the vertical temperature and contaminant distribution (Morton 1956; Mundt 1996) [17] [2]. These models present relative simple steady state solutions of the flow field characteristics in order to determine thermal comfort conditions and contaminant distribution.

The applicability of the semi-empirical relations often is restricted. For more detailed information on the flow field the full Navier-Stokes equations and the equation for conservation of heat must be solved. This technique is applied in Computational Fluid Dynamics (CFD). In CFD the equations have been discredited in order to solve the flow field numerically. Nielsen (1974) was one of the first to apply CFD for the numerical prediction of the indoor air flow [8]. Since then the technique has evolved and numerous results have indicated the wide-spread applicability of CFD for the simulation of an indoor air flow pattern. The developments in computer capacity have further enhanced the application of this type of simulations. CFD has become an increasing important tool in the prediction of the stationary indoor air flow pattern. Experience however also indicates the limitations of the current available CFD-methods, with respect to, e.g., the reliability and the sensitivity, and the necessity to validate CFD-results of typical indoor air flow patterns.

The above discussed flow modeling is focused on stationary characteristics with a view to assess indoor air quality and thermal comfort. Analysis of the energy use of a room or a building however requires information on the transient characteristics of the indoor climate. In building simulation programs (e.g. ESP-r (Clarke 1985)) the room air flow normally is modeled as a single node in an air flow network, assuming a fully mixed room [18]. As a result the effect of thermal stratification within the room on the energy use or the thermal comfort is not taken into account. A more accurate representation is possible when the room is divided into a limited number of fully-mixed sub-zones (Hensen et al. 1996) [19]. Though incorporation in a whole building air flow network is straightforward, the inter zonal flow characteristics must be pre-defined. A more rigorous analysis is possible when a CFD- program is integrated in the network model. Given the geometry and grid distribution, the flow problem then is solved from the boundary conditions presented by the nodal network.

Due to the complexity and high computing demands CFD is applied in various ways in building simulation and cooling load programs. For specific air supply systems Chen (1988) determined relations for the temperature distribution in the room, as a function of the internal heat load and the ventilation rate, from a range of simulated air flow patterns using CFD [20]. Such a relation then was incorporated in a cooling load program for further calculations. A fully integrated CFD-program in a building simulation program has been described by Negrão (1995) [21]. Negrão indicated the potential of the combined approach of CFD and whole building simulation. The main restrictions lie in the difficult convergence of the combined flow network and CFD-domain and the high computational effort required.

From the above it can be concluded that CFD in principle is applicable for unsteady state indoor air flow problems. Nevertheless, up to now only the CFD-based investigation of steady state flow and heat transfer problems in the indoor environment has proven useful and an important extension to the available options. The validity of CFD-results however remains an issue of concern given the necessary discretization and the numerical input parameters (Chen 1997) [22]. Chen (1997) indicates the necessity of an experimental validation of a flow model. The literature review described in above concludes that the number of full scale measurements of realistic indoor air flow patterns however is restricted [22].

2.4 NUMERICAL MODELS

This section briefly describes the main mathematical and numerical characteristics of a CFD fluid flow simulation. This section explains the turbulent and heat transfer numerical models used in the present study. The governing equations and boundary conditions for all studies are presented in this section. The domain is separated into small cells to form a volume mesh (or grid) using the program GAMBIT and algorithms in FLUENT are used to solve the governing equations for viscous flow, i.e. the Navier Stokes equations.

2.4.1 Governing Equations

The flows being considered involve mechanically induced flow (air entering thought a vent) and buoyant forces that drive the air motion in the domain considered. An important factor in the flow calculations is taking into consideration the buoyant forces (natural convective flow) that arise due to differences in fluid density due to temperature difference. The air flow can be considered incompressible as the velocities are low (air flows can usually be considered incompressible if the Mach number is less than roughly 0.3 or about 100m/s). Also air being a Newtonian fluid displays a linear relationship between shear and strain rate. The laws of conservation of mass (continuity) and momentum are used to describe the flow based on the assumptions discussed. Equations (2.1), (2.2), (2.3), and (2.4) below are Navier Stokes equations in the x, y and z directions and the continuity equation which describes the flow.

Momentum in x-direction

$$\frac{\partial}{\partial t}(\rho u)+\frac{\partial}{\partial x}(\rho uu)+\frac{\partial}{\partial y}(\rho vu)+\frac{\partial}{\partial z}(\rho wu)=-\frac{\partial P}{\partial x}+\mu\left(\frac{\partial^2 u}{\partial x^2}+\frac{\partial^2 u}{\partial y^2}+\frac{\partial^2 u}{\partial z^2}\right) \tag{2.1}$$

Momentum in y-direction

$$\frac{\partial}{\partial t}(\rho v)+\frac{\partial}{\partial x}(\rho uv)+\frac{\partial}{\partial y}(\rho vv)+\frac{\partial}{\partial z}(\rho wv)=$$

$$-\frac{\partial P}{\partial y}+\mu\left(\frac{\partial^2 v}{\partial x^2}+\frac{\partial^2 v}{\partial y^2}+\frac{\partial^2 v}{\partial z^2}\right)-\rho g\beta(T_\infty-T) \tag{2.2}$$

Momentum in z-direction

$$\frac{\partial}{\partial t}(\rho w)+\frac{\partial}{\partial x}(\rho uw)+\frac{\partial}{\partial y}(\rho vw)+\frac{\partial}{\partial z}(\rho ww)=-\frac{\partial P}{\partial z}+\mu\left(\frac{\partial^2 w}{\partial x^2}+\frac{\partial^2 w}{\partial y^2}+\frac{\partial^2 w}{\partial z^2}\right)$$

25

(2.3)

Continuity

$$\frac{\partial}{\partial x}(\rho u)+\frac{\partial}{\partial y}(\rho v)+\frac{\partial}{\partial z}(\rho w)=0 \tag{2.4}$$

The y-axis of the Cartesian coordinate system is aligned in the vertical direction as shown in Figure 2-1. *u*, *v*, and *w* are the velocity components in the *x*, *y*, and *z* directions respectively, ρ is the mass density, μ is the viscosity and β is the thermal expansion coefficient of air. *t* is time, T is the temperature, *P* is the pressure, and *g* is the gravitational acceleration. The Boussinesq approximation was used and therefore fluid properties were assumed constant except for the density change with temperature which leads to the buoyancy forces. The density change is assumed to be proportional to the temperature difference.

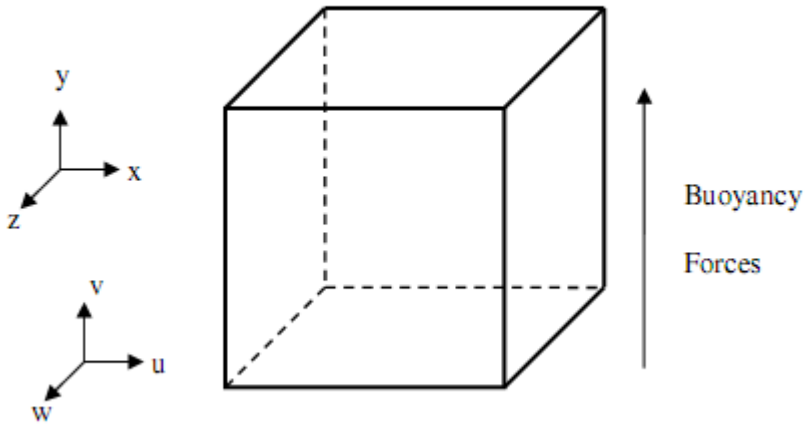

Figure 2.1: Coordinate system and control volume used in present study

The equation of continuity simply states that mass is conserved or that the net accumulation of mass in the control volume is zero in steady flow. Each term in the continuity equation represents the net mass flow through a face perpendicular to one of the respective axis.

Because the y direction equation contains a temperature dependant term, a necessary addition to the Navier Stokes equations is the energy equation. Because of the assumptions being used, the conservation of energy equation is:

$$\frac{\partial}{\partial t}(\rho c_p T)+\frac{\partial}{\partial x}(\rho u c_p T)+\frac{\partial}{\partial y}(\rho v c_p T)+\frac{\partial}{\partial z}(\rho w c_p T)=K\left(\frac{\partial^2 T}{\partial x^2}+\frac{\partial^2 T}{\partial y^2}+\frac{\partial^2 T}{\partial z^2}\right)+q''' \tag{2.5}$$

where c_p is the specific heat (J/kgK), and K is the conductivity (W/m K) of the fluid and q''' is the rate of internal heat generation.

Equations 2.1 to 2.5 describe the flow and temperature distributions. For turbulent flow, the velocity and temperature vary with time and the model that has been developed to predict turbulent flow in this study will be investigated below.

2.4.2 K-Epsilon Turbulence Model

The K-Epsilon model has become one of the most widely used turbulence models as it provides robustness, economy and reasonable accuracy for a wide range of turbulent flows. There are three versions of K-Epsilon turbulence model available in Fluent; the Standard K-Epsilon model, the RNG (renormalization group) model and the realizable model. However, only the Standard K-Epsilon model will be investigated here because it will be used in this study. The standard, RNG, and realizable models have similar form with transport equations for k and ε. The two transport equations independently solve for the turbulent velocity and length scales. The main differences between the three models are as follows;

- The turbulent Prandtl Numbers governing the turbulent diffusion of k and ε
- The generation and destruction terms in the equation for ε
- The method of calculating turbulent viscosity

Standard K-Epsilon Turbulence Model

This original model was initially proposed by Launder and Spalding (1972) [23]. For this model the transport equation for k is derived from the exact equation, but the transport for ε was obtained using physical reasoning and is therefore similar to the mathematically derived transport equation of k. The turbulent kinetic energy, k and its rate of dissipation, ε for this model are obtained by the following equations.

$$\frac{\partial}{\partial t}(\rho k)+\frac{\partial}{\partial x_i}(\rho k u_i)=\frac{\partial}{\partial x_j}\left[\left(\mu+\frac{\mu_t}{\sigma_k}\right)\frac{\partial k}{\partial x_j}\right]+G_k+G_b-\rho\varepsilon-Y_M+S_K$$

$$\frac{\partial}{\partial t}(\rho \varepsilon)+\frac{\partial}{\partial x_i}(\rho \varepsilon u_i)=\frac{\partial}{\partial x_j}\left[\left(\mu+\frac{\mu_t}{\sigma_\varepsilon}\right)\frac{\partial \varepsilon}{\partial x_j}\right]+C_{1\varepsilon}\frac{\varepsilon}{k}(G_k+C_{3\varepsilon}G_b)-C_{2\varepsilon}\rho\frac{\varepsilon^2}{k}+S_\varepsilon$$

where G_k represents the generation of turbulent kinetic energy the arises due to mean velocity gradients, G_b is the generation of turbulent kinetic energy that arises due to buoyancy, and Y_M represents the fluctuating dilation in compressible turbulence that contributes to the overall dissipation rate. S_ε and S_k are source terms defined by the user.

$C_{1\varepsilon}$, $C_{2\varepsilon}$ and C_μ are constants that have been determined experimentally and are taken to have the following values;

$$C_{1\varepsilon}=1.44,\ C_{2\varepsilon}=1.92,\ C_\mu=0.09$$

σ_k and σ_ε are turbulent Prandtl numbers for the turbulent kinetic energy and its dissipation rate. These have also been derived experimentally and are defined as follows.

$$\sigma_k=1.0,\ \sigma_\varepsilon=1.3$$

The turbulent (or eddy) viscosity at each point is related to the local values of turbulent kinetic energy and its dissipation rate by;

$$\mu_t = \rho C_\mu \frac{k^2}{\varepsilon}$$

where C_μ is constant and defined above.

The term for the production of turbulent kinetic energy G_k is common in many of the turbulence models studied and is defined as

$$G_k = -\rho \overline{u_i' u_j'} \frac{\partial u_j}{\partial x_i}$$

The modulus of mean rate-of-strain tensor, S is defined as

$$S = \sqrt{2 S_{ij} S_{ij}}$$

The generation of turbulent kinetic energy that arises due to buoyancy, G_b is defined as follows

$$G_b = \beta g_i \frac{\mu_t}{\mathrm{Pr}_t} \frac{\partial T}{\partial x_i}$$

As the present study uses relatively low velocities, the dilation dissipation term, Y_M which accounts for turbulence from compressibility effects is defined as

$$Y_M = 2\rho \varepsilon M_t^2$$

CHAPTER 3

METHODOLOGY

3.1 PROJECT WORKS

To start the project the author shall identify the list of work that will be done during the project. In addition, the author must get familiarize with the software to be used in carrying this project. Figure 3.1 below shows the methodology planned for the implementation of this project.

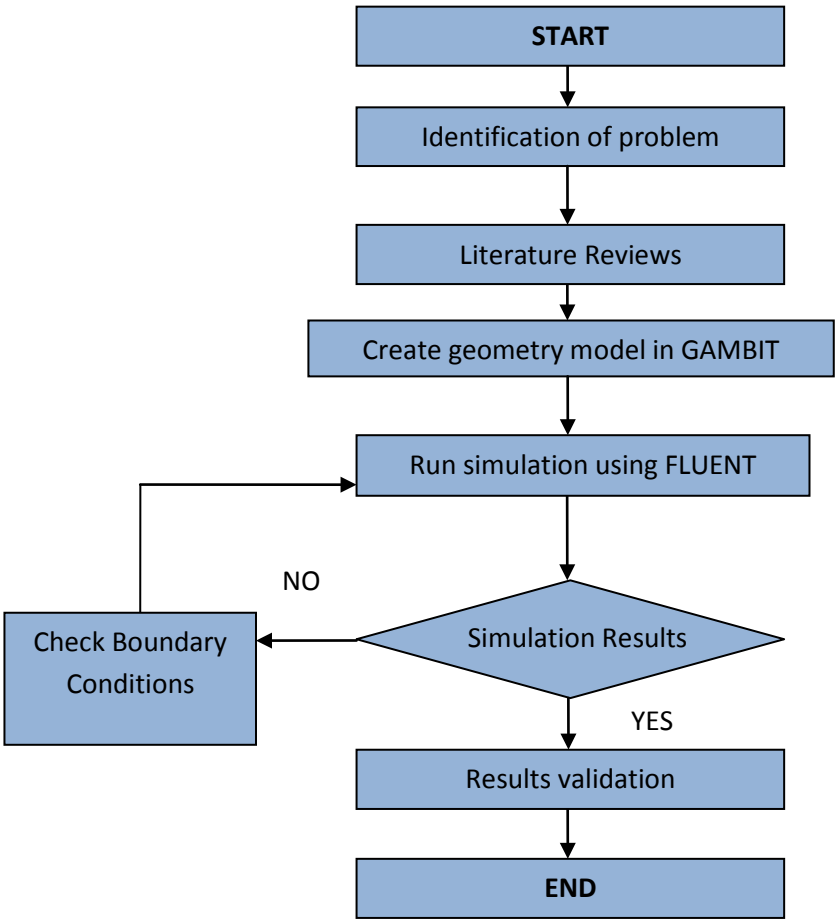

Figure 3.1: Flow Chart for the Study

3.2 GANTT CHART AND MILESTONE

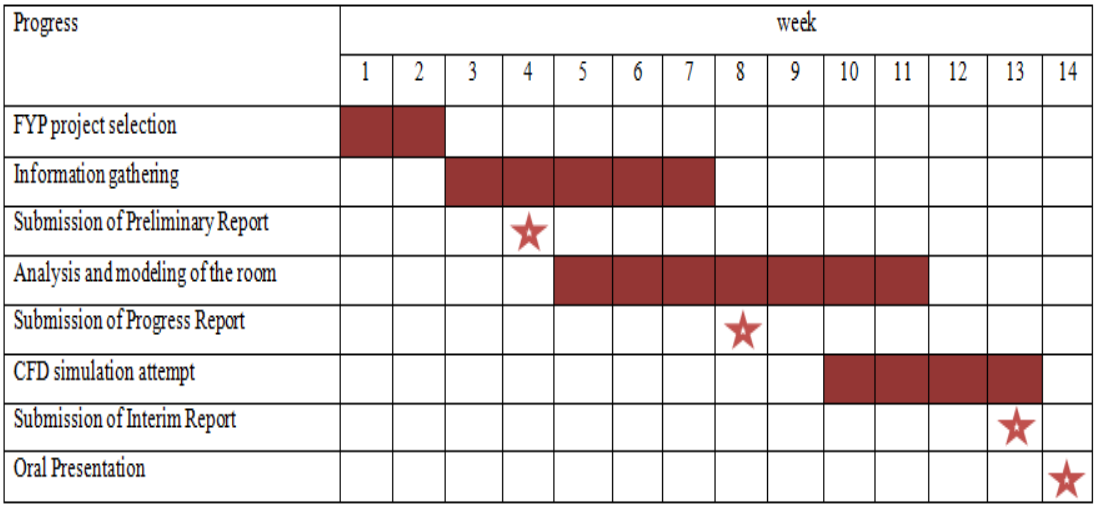

Figure 3.2: Gantt chart for FYP1

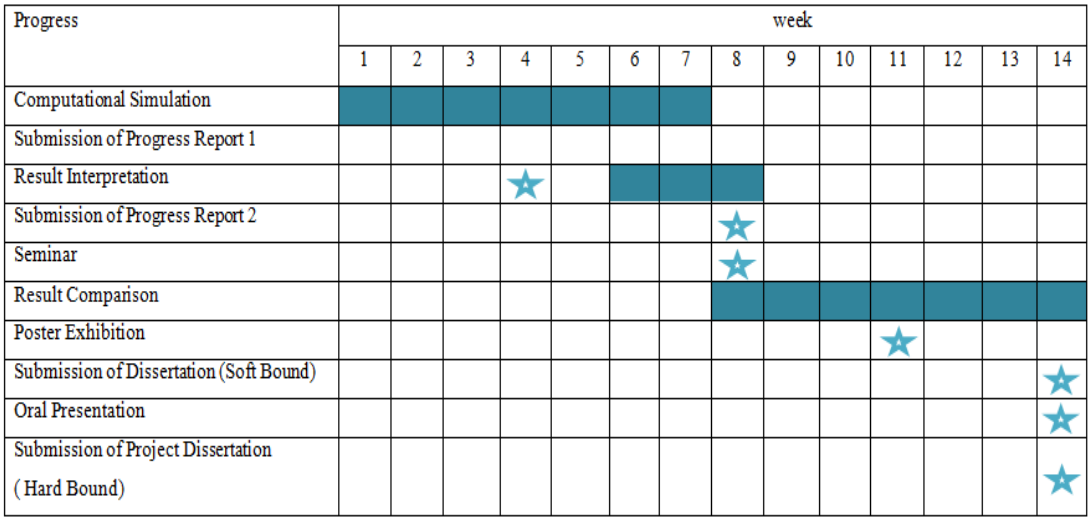

Figure 3.3: Gantt chart for FYP2

3.3 TOOLS / EQUIPMENTS REQUIRED

The main tool and equipment required in this Final Year Project research is a computer with Windows operating system together with the programs such as GAMBIT v2.4 and FLUENT v6.3 for simulation works and Microsoft Office for documentation purpose.

3.4 CFD BACKGROUND

Computational fluid dynamics (CFD) uses numerical methods to solve and analyze problems that involve fluid flows. The governing equations discussed above have been solved with respect to the specified boundary conditions using the finite volume method as implemented in the commercial CFD code FLUENT.

There are three components in CFD analysis; the pre-processor, the solver, and the post-processor. Preprocessor is defined as a program that processes input data to produce output that is used as an input to the processor. In the present study, the preprocessor being used is Gambit 2.4. Gambit was used to create the geometry of the system being considered and subdivide the domain into elements which as a whole constitute the mesh or grid. The solution of the flow is later solved at the center of each of these volumes by the solver. The preprocessor also defines general surface types (for example - inlet/outlet areas) to regions of the domain. Finally the post-processor is a tool that allows the interpretation of the solution in the form of graphs, plots, and charts. FLUENT is used for both the solver and the post-processor in the present work. Microsoft Excel is also used as a post processor for making graphs and charts to be presented in this report.

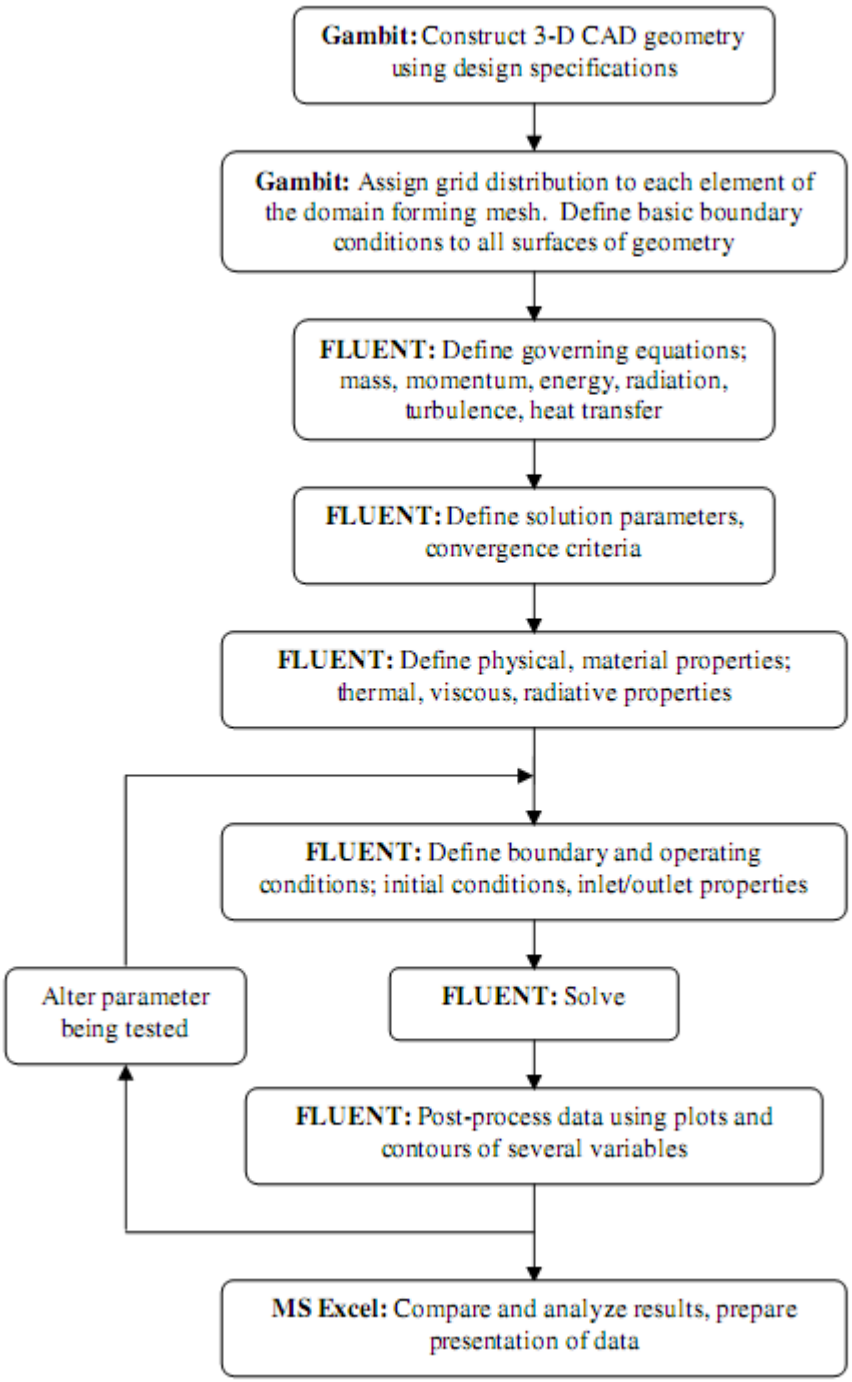

Figure 3.4: Flow Chart of Method Used for CFD Application

3.5 MODELING GEOMETRY USING GAMBIT

The room is modeled using GAMBIT with following dimensions.

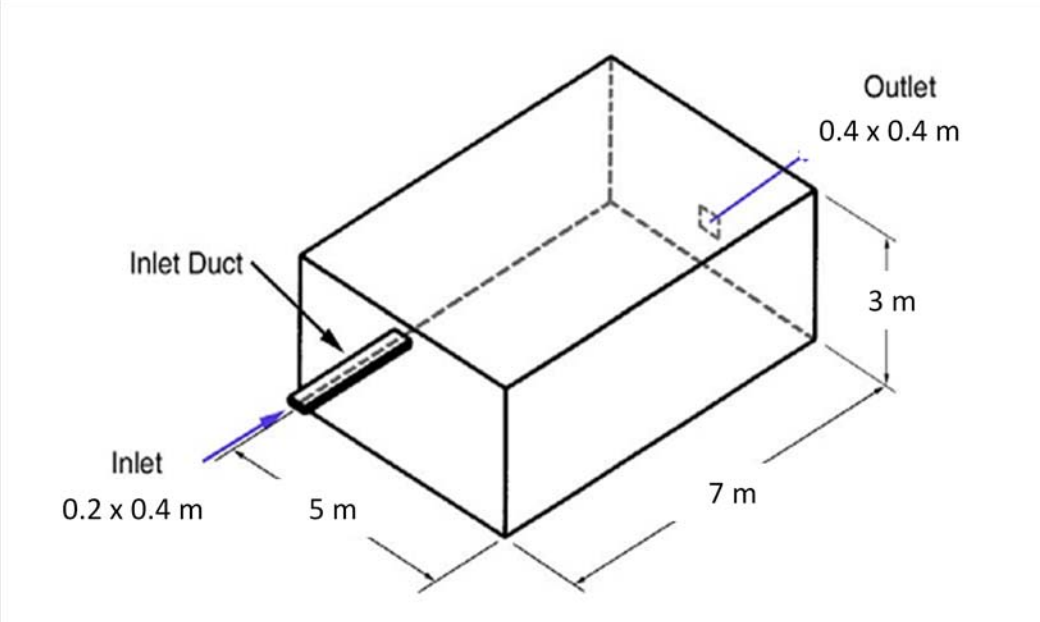

Figure 3.5: Room Geometry

The height of the inlet and the outlet from the floor is 2.6m and 0.2m.

Gambit version 2.4 software was used to mesh the geometry for the simulations and to setup boundary conditions. A hexahedral mesh was employed on the scaled room geometry. A total of 105000 elements were created using submap type and 0.1 interval size spacing. Figure 3.6 and Figure 3.7 displays the mesh generated in Gambit for the geometry of the room model.

The boundary of the diffuser inlet (blue shaded) is set to be 'VELOCITY INLET', outlet (red shaded) is set to be 'PRESSURE OUTLET' and the other faces are set as 'WALL'.

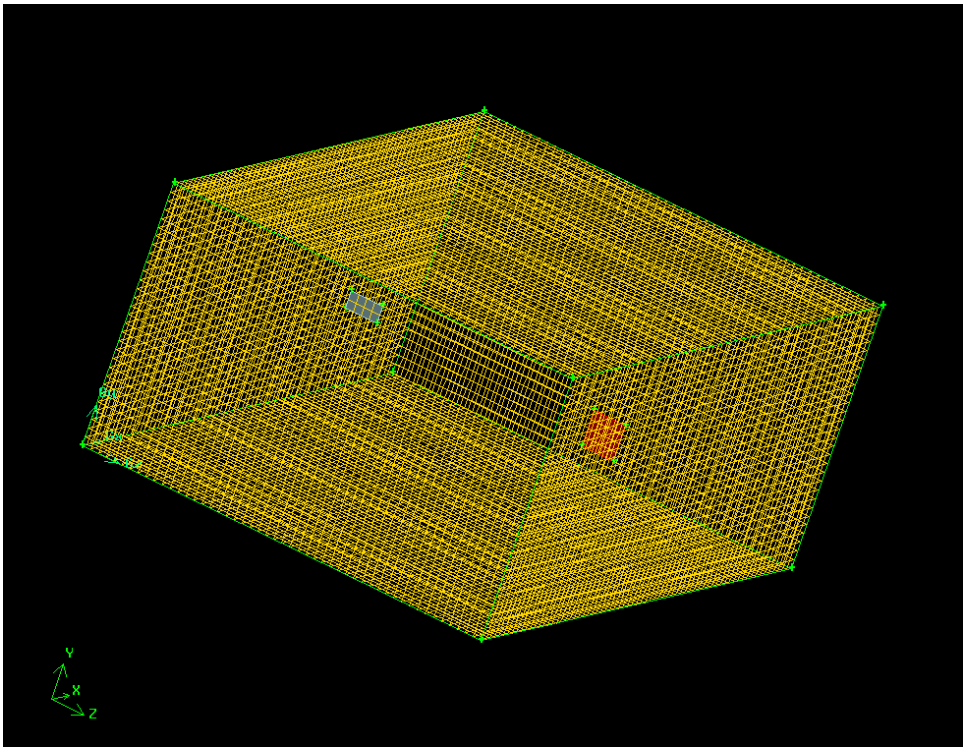

Figure 3.6: Meshed Geometry for the Room

3.6 SOLVING PROBLEM USING FLUENT

The numerical model is based on the following assumptions:

- the flow is steady, turbulent and three-dimensional
- the flow is single phase, i.e., the effects of dust particles and/or water vapor have been neglected
- the velocity is uniform over the vent inlet
- the air properties are constant, except for the density change with temperature, which has been treated using the Boussinesq Approximation.

The pressure based solver or formerly known as segregated solver was used in this simulation. Air is selected as *Fluid* Materials and to treat it following Boussinesq Approximation, certain values for air properties are used:

Temperature, T = 300K
Density, ρ = 1.177 kg/m^3
Specific heat capacity, C_P = 1004.9 J/kg.K
Thermal conductivity = 0.0262 W/m.K
Dynamic viscosity, μ = 1.846e-5 kg/ms
Thermal expansion coefficient, β = 0.00343

Turbulence model used for this simulation is Standard k- ε with enhanced wall treatment. All the values are taken by default properties provided in the FLUENT v6.3. Gravity is acting on the y-direction. The inlet air temperature is 290K meanwhile the wall and operating temperature is set to 300K. The uniform inlet velocity was given an initial value of 0.5 m/s for the first case and 1.5m/s for the second case. Convergence criteria were set at 10^{-4} for each residual within Fluent.

A ~2.0 GHz AMD Athlon™ 64 X2 Dual Core Processor personal computer running Windows 7, with 2 GB of RAM, was used to perform the simulations. The standard k-ε simulation required approximately 4000 iterations to achieve convergence. Each simulation required about 2 hours of computing time to complete.

CHAPTER 4

RESULT AND DISCUSSION

Numerical models have been developed to allow the study of the stationary and transient characteristics of an air flow pattern with regard to energy use, indoor air quality and thermal comfort. From this numerical method, hopefully the influence of diffuser position and air flow variation to the room temperature distribution can be analyzed.

There are two parts involved in this simulation where the first part is using 0° diffuser angle and second part is using 45° diffuser angle in order to show the influence of the diffuser position. Each part has two cases to show the influence of airflow variation. The velocity is varied for each case which is 0.5m/s for case 1 and 1.5m/s for case 2.

4.1 RESULT

Although results were obtained in three dimensions throughout the room, only one vertical plane within the room are selected here for the comparison and analysis purpose. This is because person is assumed located in the middle of the room. The xy plane is at the center of the room, at z = 2.5m.

The first parameter chosen for comparison is velocity, and velocity vectors normalized to equal length are used so that the direction of flow can easily be seen, even though the velocity magnitudes at different locations were not the same. Contour plots of velocity ranging from v = 0 – 0.5m/s for case 1 and v = 0 – 1.5m/s for case 2 for each part are shown below. The contour plots show the velocity magnitude for the x and y planes only.

The second parameter chosen for comparison is temperature, and contour plots of temperature for part 1 and part 2 is shown for each case. Each of the contour plot of temperature has same scale, ranging from T = 290 – 300K (17 - 27°C).

For the analysis part, the horizontal and vertical temperature distribution in the middle of the room will be plotted. The horizontal temperature distribution will be plotted along the x-axis taken the height of 1.1m, considering the person in sitting position respectively. While for the vertical temperature distribution, it will be plotted from the floor to the ceiling in the middle of the room.

Part 1

Figure 4.1 shows the overview of airflow in the room. Movements and directions of the air is indicated by the arrows.

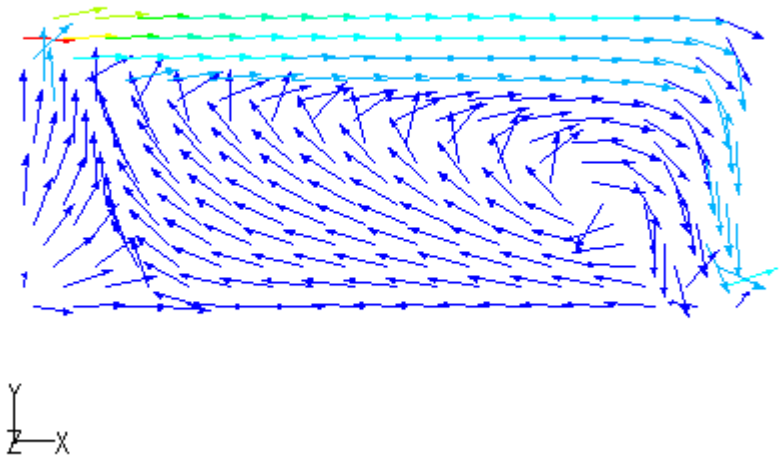

Figure 4.1: Vector of Velocity

Figure 4.2 – Figure 4.5 below shows the contour of the velocity magnitude and temperature distribution in the room for both cases.

Figure 4.6 shows the temperature distribution of the four air flows along the x-axis and Figure 4.7 shows the temperature distribution along the y-axis.

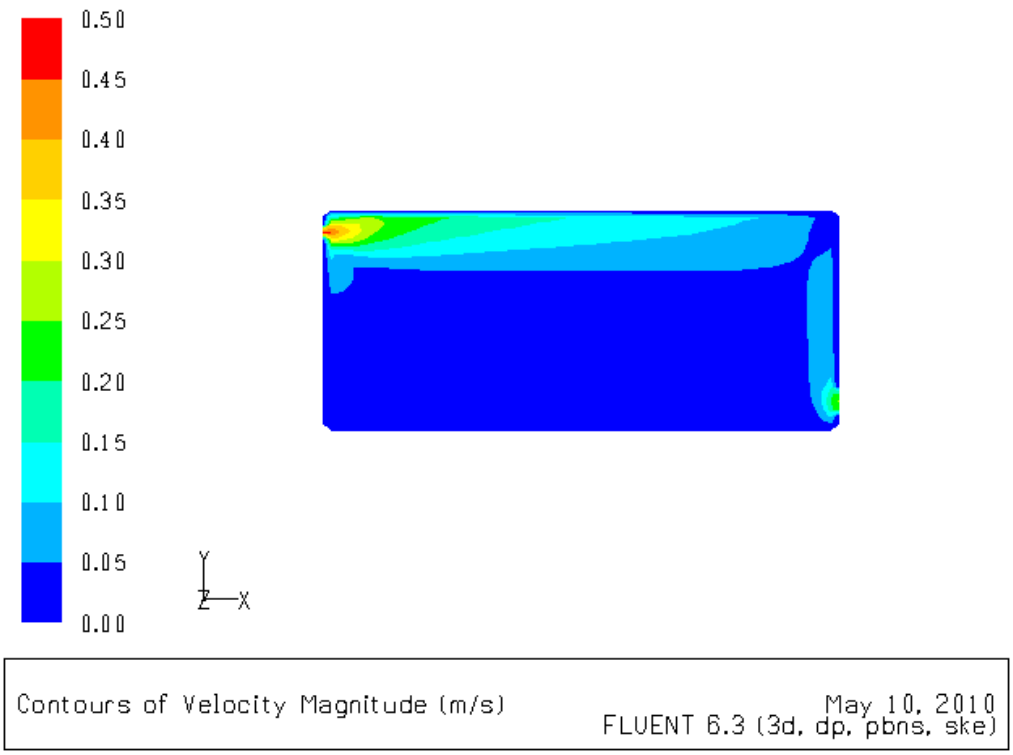

Figure 4.2: Contour of Velocity Magnitude at v = 0.5m/s

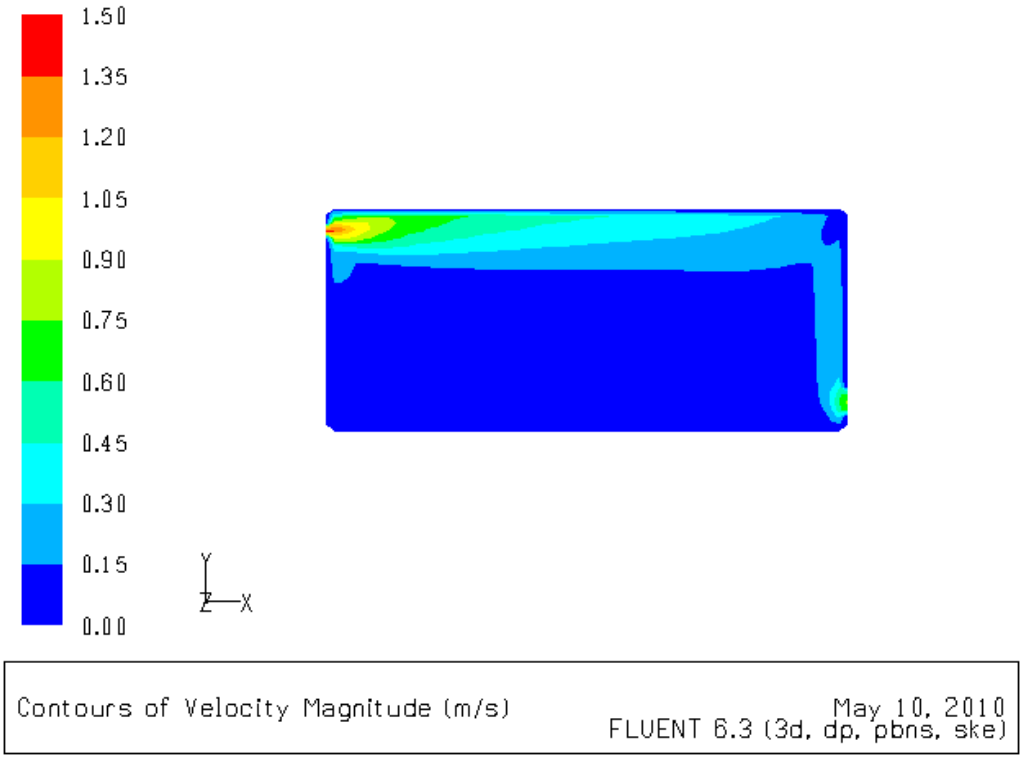

Figure 4.3: Contour of Velocity Magnitude at v = 1.5m/s

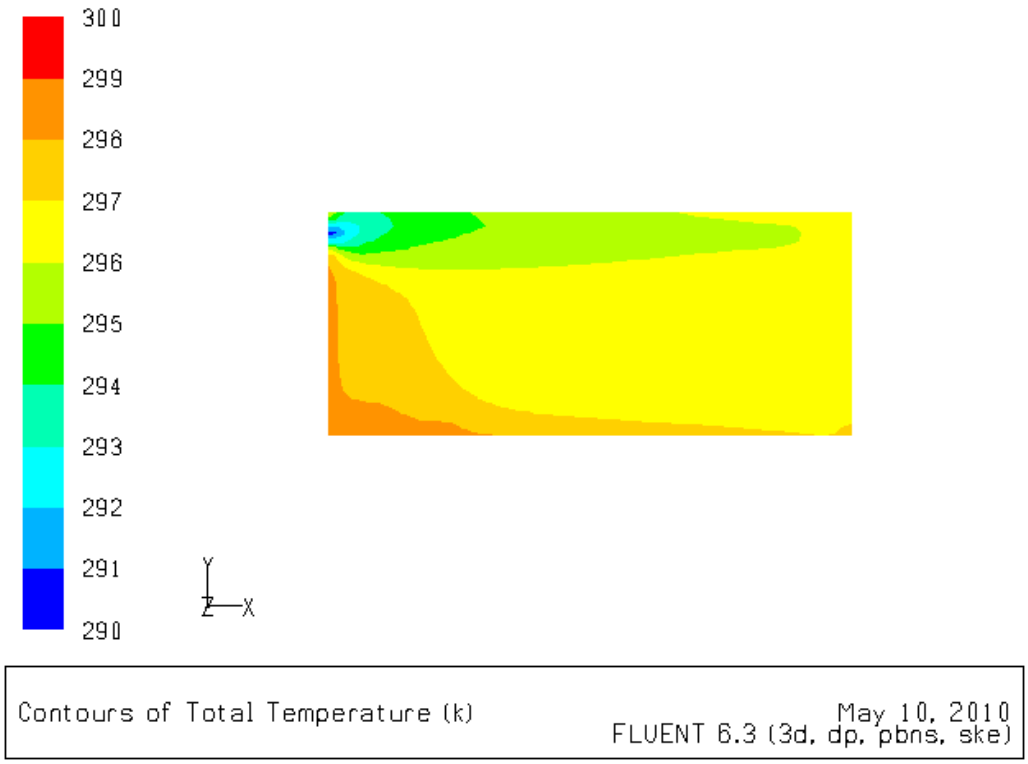

Figure 4.4: Contour of Total Temperature at v = 0.5m/s

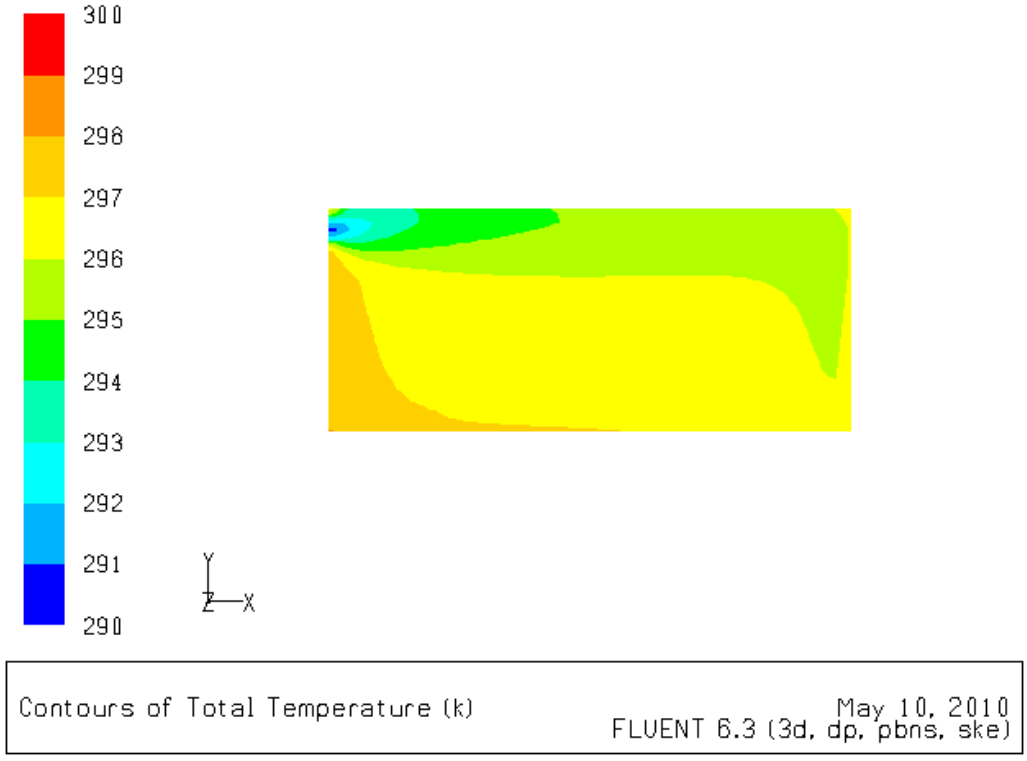

Figure 4.5: Contour of Temperature at v = 1.5m/s

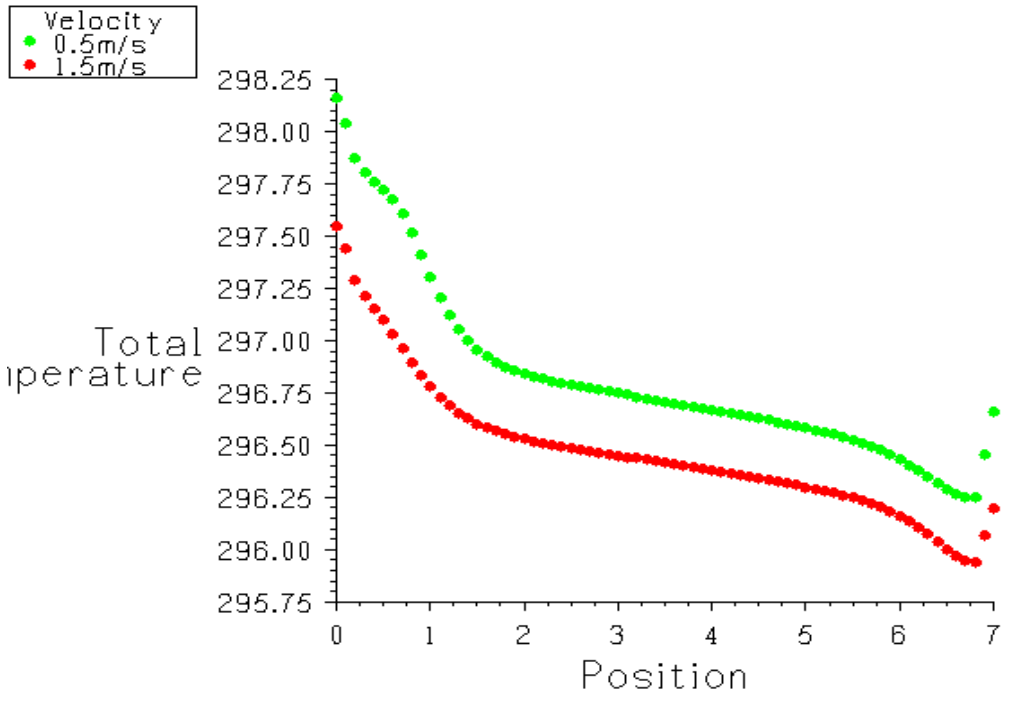

Figure 4.6: Temperature Distribution Along the x-axis

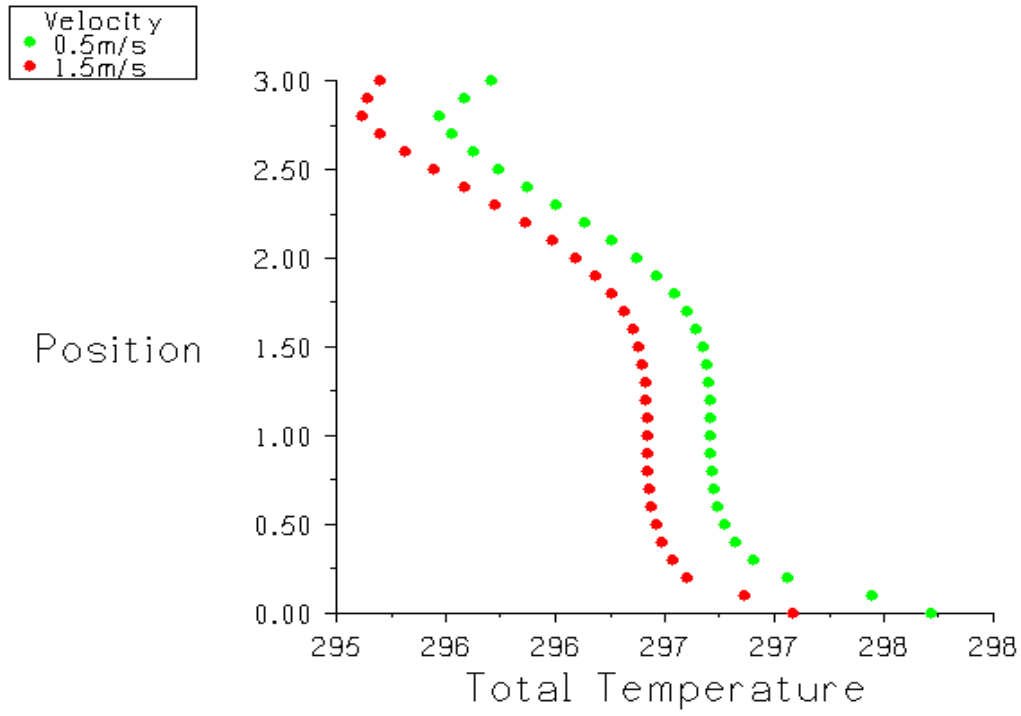

Figure 4.7: Temperature Distribution Along the y-axis

Part 2

Figure 4.8 shows the overview of airflow in the room. Movements and directions of the air is indicated by the arrows.

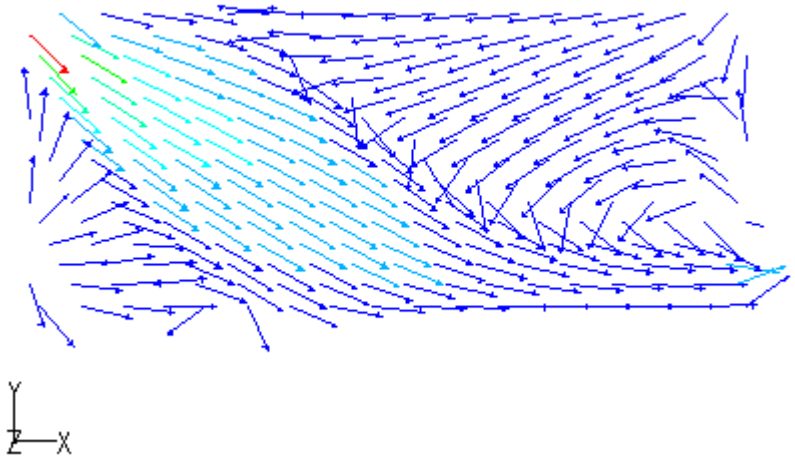

Figure 4.8: Vector of Velocity

Air exits the diffuser at 45° angle and moving in the following direction. Air is circulating in the room. Air is then moving downward due to the gravity force acting in y-direction.

Figure 4.9 – Figure 4.12 below shows the contour of the velocity magnitude and temperature distribution in the room for both cases.

Figure 4.15 shows the temperature distribution of the four air flows along the x-axis and Figure 4.16 shows the temperature distribution along the y-axis.

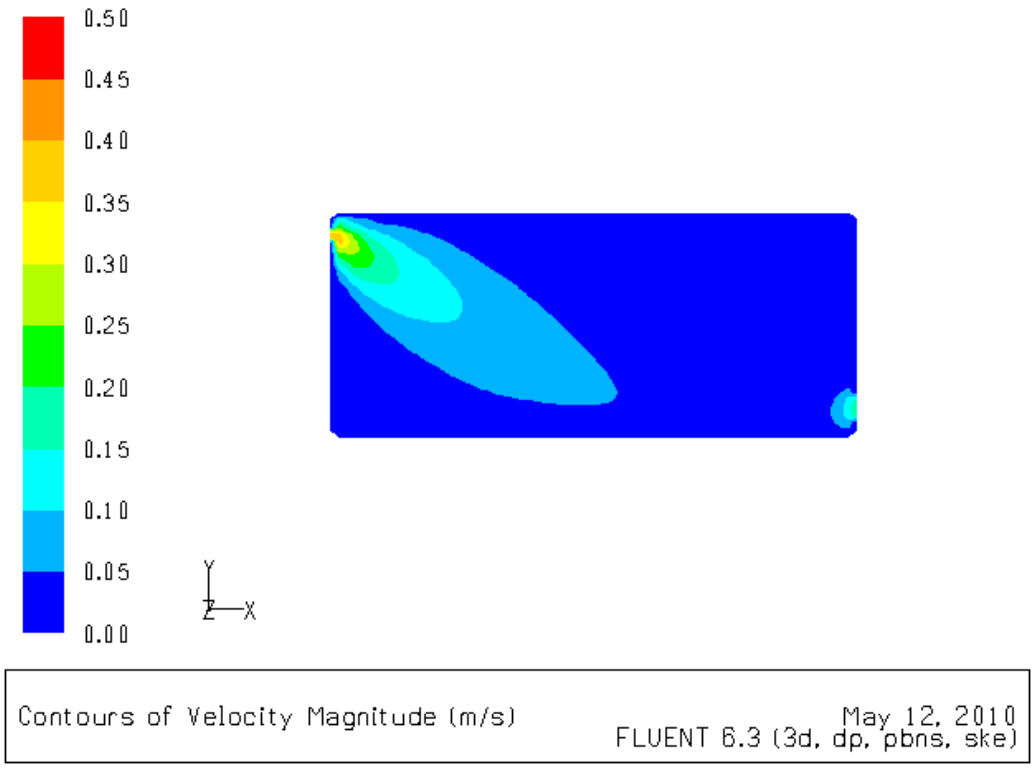

Figure 4.9: Contour of Velocity Magnitude at v = 0.5m/s

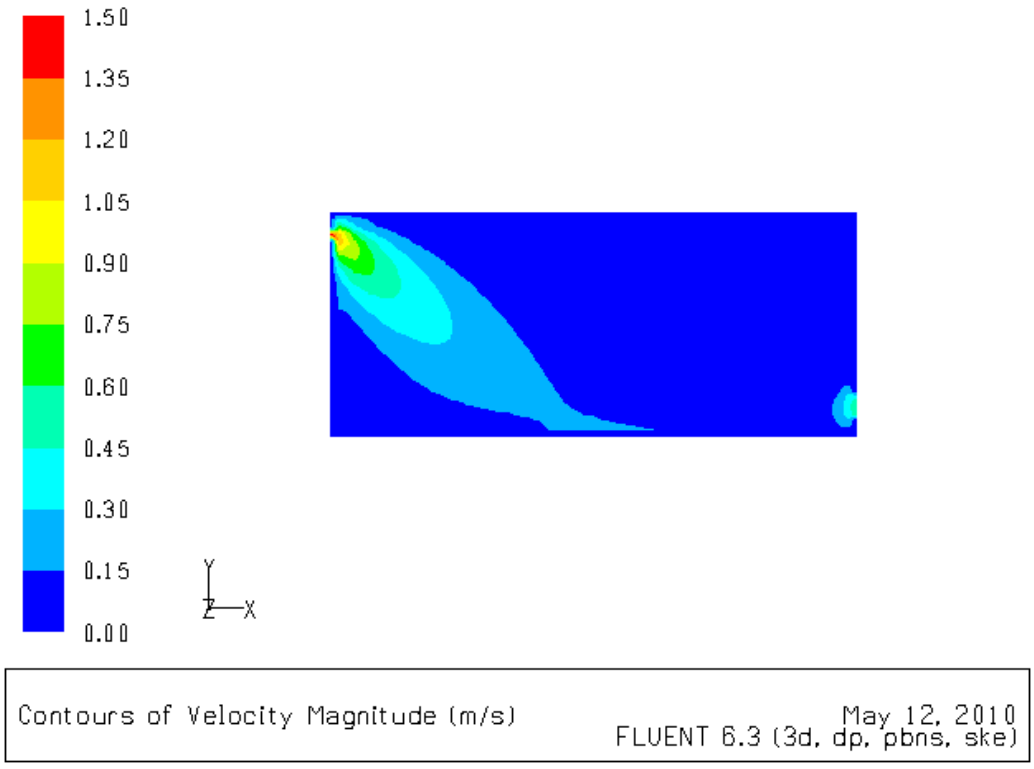

Figure 4.10: Contour of Velocity Magnitude at v = 1.5m/s

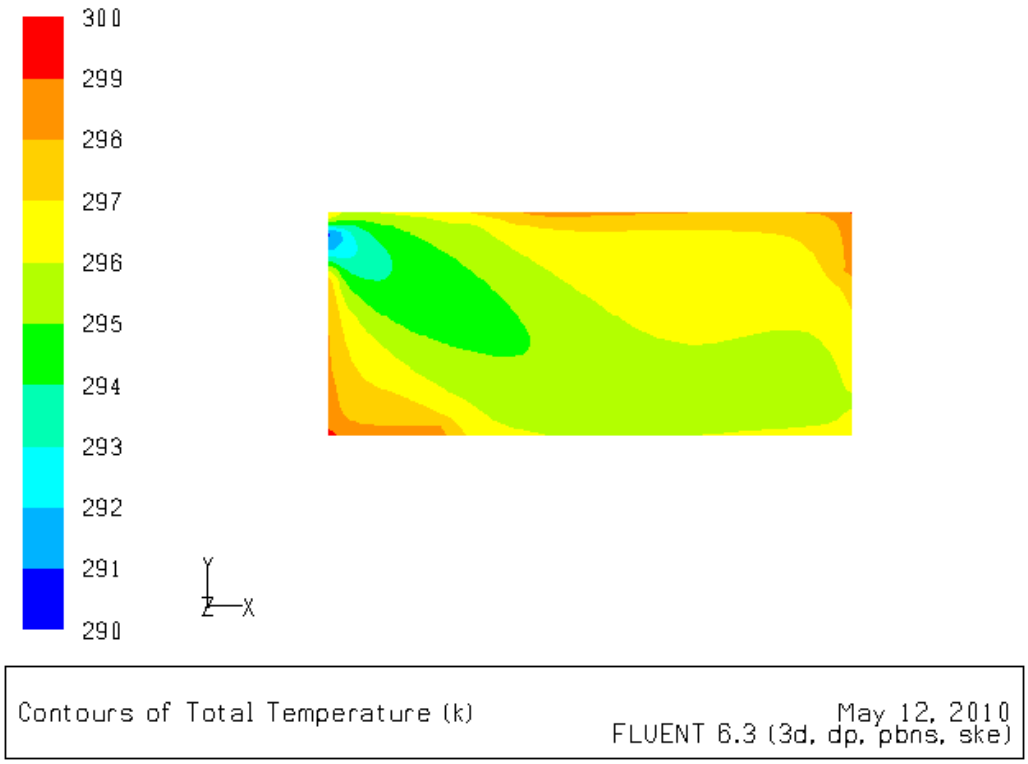

Figure 4.11: Contour of Total Temperature at v = 0.5m/s

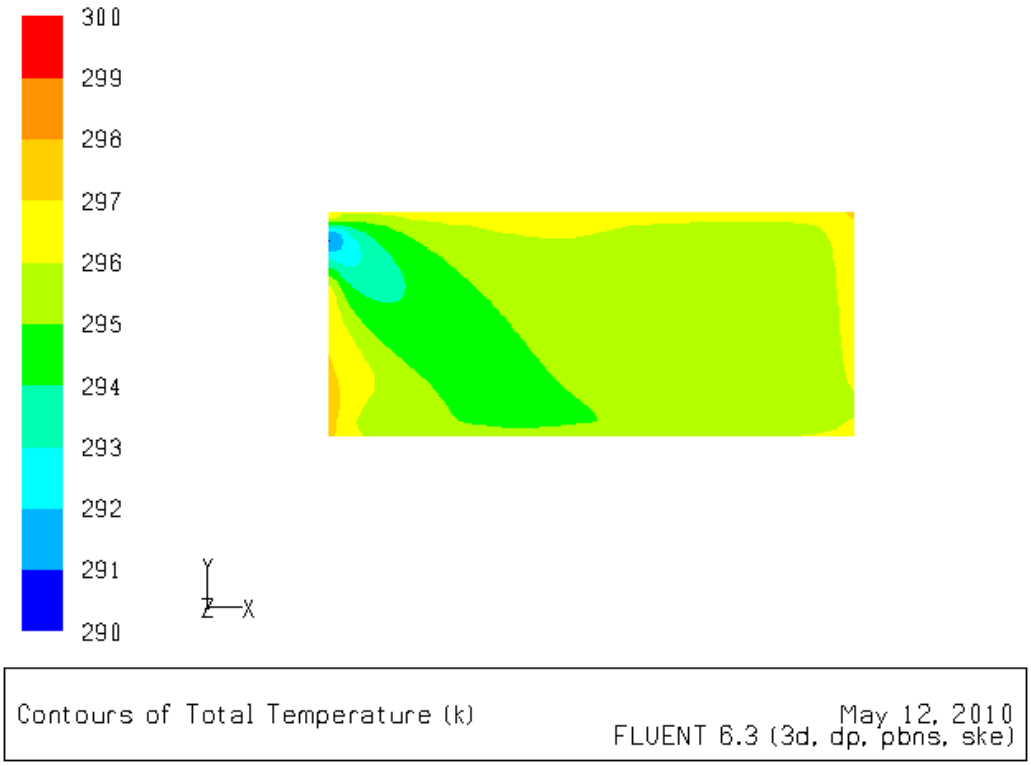

Figure 4.12: Contour of Temperature at v = 1.5m/s

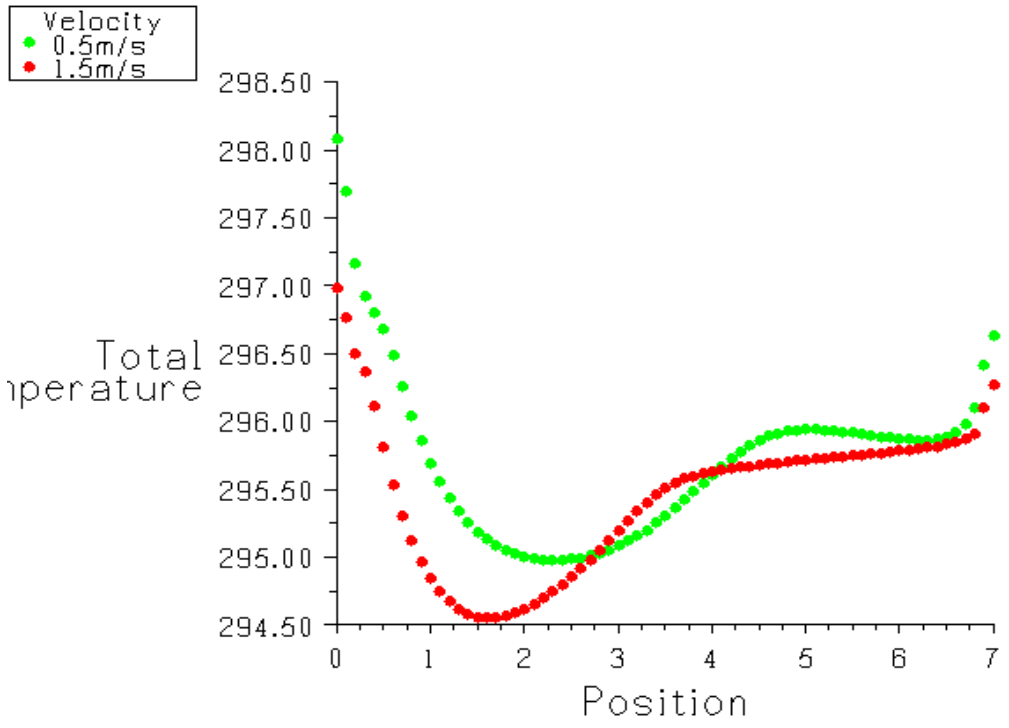

Figure 4.13: Temperature Distribution Along the x-axis

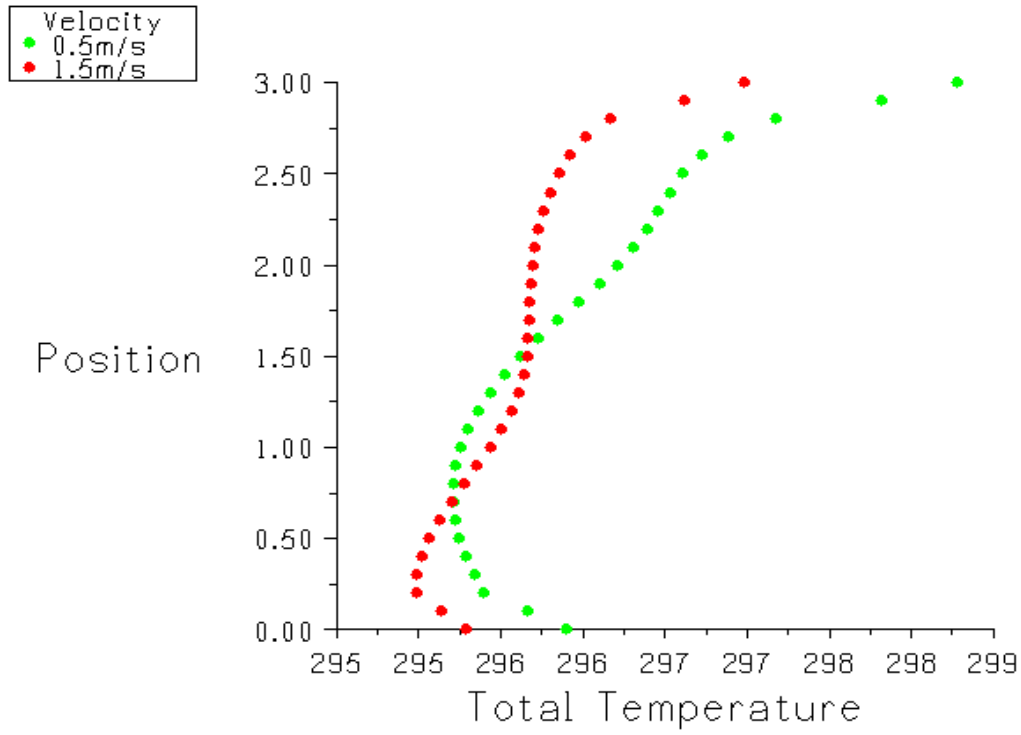

Figure 4.14: Temperature Distribution Along the y-axis

4.2 ANALYSIS

From the results above, the influence of diffuser position and airflow velocity variation to the temperature distribution within the room can clearly been seen by observing velocity and temperature contours and also the graphs in the figures shown in the section.

For the analysis part, the horizontal and vertical temperature distribution in the middle of the room will be plotted. The horizontal temperature distribution will be plotted along the x-axis taken the height of 1.1m, considering the person in sitting position respectively. While for the vertical temperature distribution, it will be plotted from the floor to the ceiling in the middle of the room.

There are four different air flows with different diffuser angle and velocity will be analyzed in this section. The first flow with 0° diffuser angle and 0.5m/s velocity, second flow with 0° diffuser angle and 1.5m/s velocity, the third flow with 45° diffuser angle and 0.5m/s and the fourth flow with 45° diffuser angle and velocity of 1.5m/s.

Figure 4.15 shows the temperature distribution of the four air flows along the x-axis and Figure 4.16 shows the temperature distribution along the y-axis.

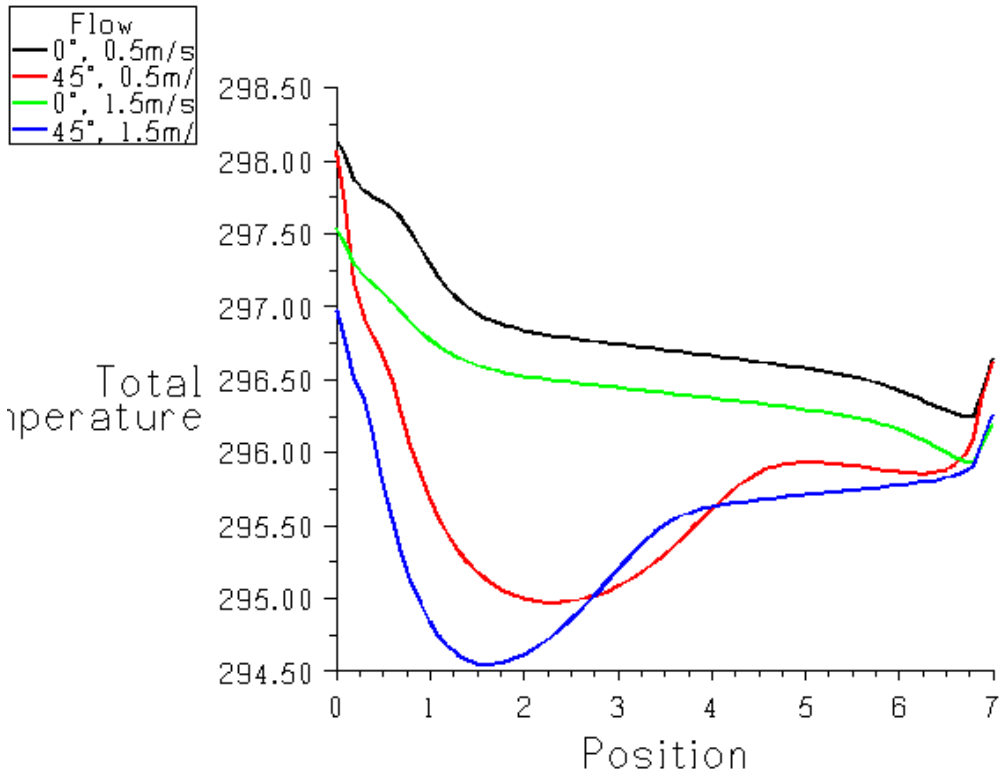

Figure 4.15: Temperature Distribution Along the x-axis

Air flow with 0° diffuser angle and different velocity has merely the same temperature distribution along the x-axis with height of 1.1m from the floor. However, air flow with velocity of 1.5m/s has cooler temperature distribution with the highest and lowest temperature is approximately 297.5K and 296K than the one with 0.5m/s velocity with highest and lowest temperature of 298.1K and 296.25K.

For air flow with 45° diffuser angle and different velocity also has merely the same temperature distribution along the x-axis. However, air flow with velocity of 1.5m/s has cooler temperature distribution with the highest and lowest temperature is approximately 297K and 294.5K than the one with 0.5m/s velocity with highest and lowest temperature of 298.1K and 295K except at the position 3 - 4m where the air flow with velocity of 0.5m/s has lower temperature.

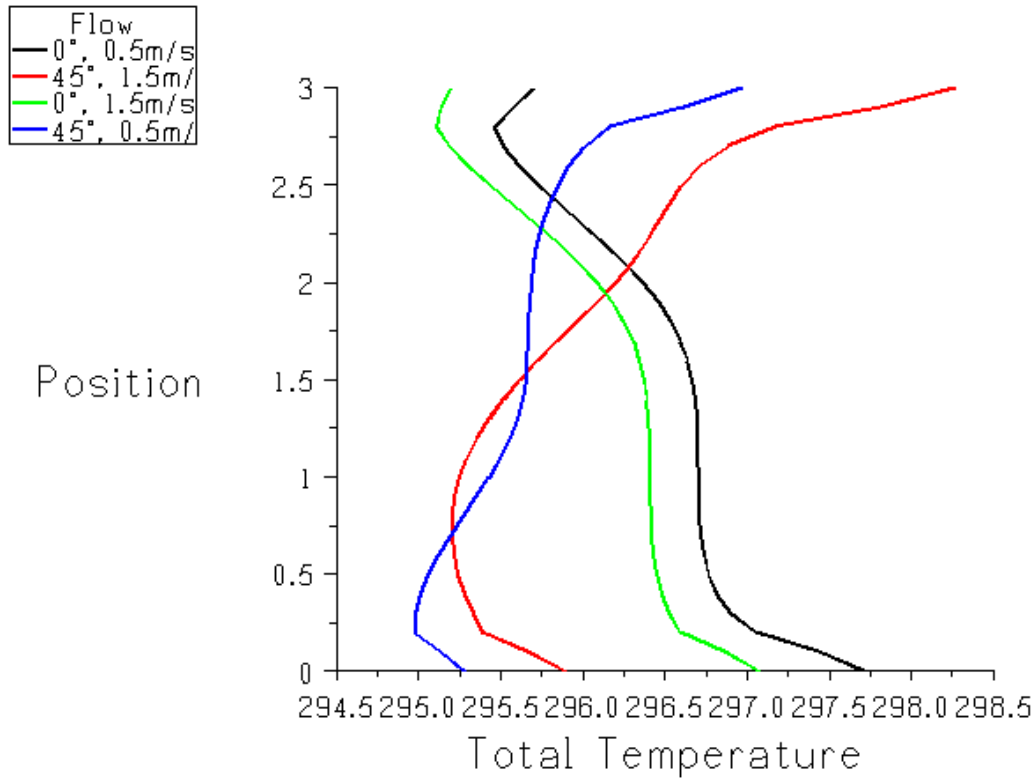

Figure 4.16: Temperature Distribution Along the y-axis

The vertical temperature distribution in the middle of the room for air flow with 0° diffuser angle and different velocity is merely the same. However, air flow with velocity of 1.5m/s has cooler temperature distribution with the highest and lowest temperature is approximately 297K and 295.25K than the one with 0.5m/s velocity with highest and lowest temperature of 297.75K and 295. 5K.

For air flow with 45° diffuser angle and different velocity also has merely the same vertical temperature distribution. However, air flow with velocity of 1.5m/s has cooler temperature distribution with the highest and lowest temperature is approximately 297K and 295K than the one with 0.5m/s velocity with highest and lowest temperature of 298.25K and 295.25K except at the height of 0.5 – 1.5m where the opposite thing was happened.

CHAPTER 5

CONCLUSION AND RECOMMENDATION

This research has investigated the temperature distribution within the room. Throughout the research period all the information was gathered from all reliable resources such as technical proceedings, journals and online resources. The main focus of this research is to show the influence of diffuser position and air flow variation to the temperature distribution in a room. Therefore the knowledge of heat transfer and fluid dynamics has been fully utilized to conduct the research. The research is conducted by simulating the turbine blade cooling process by using CFD software.

5.1 CONCLUSION

In this work the temperature distribution in a room is simulated. Numerical analysis based on finite volume method is used to solve three dimensional unsteady flow resulting temperature distributions and air velocity field for variation of diffuser position and air flow velocity. Analysis shows strong influence of diffuser position and air flow velocity to the temperature distribution.

Air flow with 45° diffuser angle and velocity of 1.5m/s has the lowest temperature distribution within the room. However, at height of 1.1m, where the person is considering in sitting position, temperature distribution of air flow with 45° diffuser angle and 0.5m/s is lower than the one with 1.5m/s in the middle of the room.

The best option under this condition is air flow with 45° diffuser angle and velocity of 0.5m/s because the temperature is lower at the person's sitting position and the person might feel a little draft if using velocity of 1.5m/s.

5.2 RECOMMENDATION

Although the project is completed and the objectives are achieved, the measurement result is still needed for validation purpose.

REFERENCES

[1] Carrier Air Conditioning Company. 1965. *Handbook of Air Conditioning System Design*, 4th edition, McGraw-Hill, New York, USA.

[2] Mundt, E. 1996. *The Performance of Displacement Ventilation Systems*, thesis, Royal Institute of Technology Building Services Engineering, Stockholm, Sweden.

[3] Brohus, H. 1997. *Personal Exposure to Contaminant Sources in Ventilated Rooms*, thesis, Aalborg University, Aalborg, Denmark.

[4] Benzinger, T.H. 1979. The Physiological basis for thermal comfort, *Indoor Climate*, ed. P.O.Fanger and O.ValbjØrn, pp.441-476, Danish Building Research Institute, Copenhagen, Denmark.

[5] Hawkes, D. 1996. *The Environmental Tradition*, E&FN Spon, London, Great Britain.

[6] Bauman, F., Arens, E., Fountain, M., Huizenga, C., et al. 1994. *Localized thermal distribution for office buildings*, final report - phase III, Center for Environmental Design Research, University of California, Berkeley, USA.

[7] Bauman, F.S. and Arens, E.A. 1996. *Task/Ambient conditioning systems: Engineering and application guidelines*, CEDR-13-96, University of California, Berkeley, USA.

[8] Nielsen, P.V. 1974. *Flow in Air Conditioned Rooms*, thesis, Nordberg DK.

[9] Cheesewright, R. and Ziai, S. 1986. *Distributions of temperature and local heat-transfer rate in turbulent natural convection in a large rectangular cavity*, Proc. 8th Int. Heat Transfer Conf.

[10] Thorsauge, J. 1982. Air-velocity fluctuations in the occupied zone of ventilated spaces, *ASHRAE Transactions*, vol. 88 part 2, 753-764.

[11] Hanzawa, H., Melikov, A.K. and Fanger, P.O. 1987. Airflow characteristics in the occupied zone of ventilated spaces, *ASHRAE Transactions*, vol.93 part 1, pp.524-539.

[12] Melikov, A.K., Hanzawa, H. and Fanger, P.O. 1988. Airflow characteristics in the occupied zone of heated spaces without mechanical ventilation, *ASHRAE Transactions*, vol. 94 part 1, pp.52-70.

[13] Melikov, A.K., Langkilde, G. and Derbiszewski, B. 1990. Airflow characteristics in the occupied zone of rooms with displacement ventilation, *ASHRAE Transactions*, vol. 96 part 1, 555-563.

[14] Lemaire, A.D. 1992. *Room Air and Contaminant Flow - Evaluation of computational methods*, Subtask-1 Summary report, IEA Annex 20 'Air Flow Patterns within Buildings', Delft, The Netherlands.

[15] Dantec. 1985. *54N50 Low Velocity Flow Analyzer mark II*, Dantec Electronik, Denmark.

[16] Crommelin, R.D. and Dubbeld, M. 1976. Modified anemometers for indoor climate research, *Journal of Physics E: Scientific Instruments*, vol.9, pp.1005-1009.

[17] Morton, B.R., Taylor, G.F.R.S. and Turner, J.S. 1956. *Turbulent gravitational convection from maintained and instantaneous sources*, Proc. Roy. Soc. London, vol.234 A, pp.1-23.

[18] Clarke, J.A. 1985. *Energy Simulation in Building Design*, Adam Hilger Ltd., Bristol, United Kingdom.

[19] Hensen, J.L.M., Hamelinck, M.J.H. and Loomans, M.G.L.C. 1996. *Modelling approaches for displacement ventilation in offices,* Proc. Roomvent'96, vol.2, pp.467-474, Yokohama, Japan.

[20] Chen, Q. 1988. *Indoor Airflow, Air Quality and Energy Consumption of Buildings*, thesis, Delft University of Technology, Delft, The Netherlands.

[21] Negrão, C.O.R. 1995. *Conflational of Computational Fluid Dynamics and Building Thermal Simulation,* thesis, University of Strathclyde, Glasgow, Scotland.

[22] Chen, Q. 1997. *Computational Fluid Dynamics for HVAC: Successes and Failures,* ASHRAE Transactions, vol.103 part 1, pp.178-187.

[23] Launder, B. E., Spalding, D. B. 1972. *Lectures in Mathematical Models of Turbulence*, Academic Press.